
Assessment of the ^{18}F -Labeled PET Tracer LMI1195 for Imaging Norepinephrine Handling in Rat Hearts

Takahiro Higuchi^{1,2}, Behrooz H. Yousefi^{1,3}, Franz Kaiser², Florian Gärtner¹, Christoph Rischpler¹, Sybille Reder¹, Ming Yu⁴, Simon Robinson⁴, Marcus Schwaiger¹, and Stephan G. Nekolla¹

¹Nuklearmedizinische Klinik und Poliklinik, Klinikum rechts der Isar, Technische Universität München, Munich, Germany;

²Comprehensive Heart Failure Center/Nuklearmedizinische Klinik und Poliklinik, Universitätsklinikum Würzburg, Würzburg, Germany; ³Pharmaceutical Radiochemistry, Technische Universität München, Garching, Germany; and ⁴Discovery Research, Lantheus Medical Imaging, North Billerica, Massachusetts

A novel ^{18}F -labeled tracer, LMI1195 (*N*-[3-bromo-4-(3- ^{18}F -fluoropropoxy)-benzyl]-guanidine), is being developed for sympathetic nerve imaging; its high specificity for neural uptake-1 mechanism has previously been demonstrated in cell associative studies and in rabbit and nonhuman primate studies assessing heart uptake. The aim of this study was to investigate the mechanisms of ^{18}F -LMI1195 cardiac uptake in the rat, which is known to contain norepinephrine uptake mechanisms beyond uptake-1. **Methods:** Tracer accumulation in the heart was studied over time after intravenous administration of ^{18}F -LMI1195 in healthy male Wistar rats by quantitative *in vivo* PET imaging. The uptake mechanism was assessed by pretreatment with the nonselective norepinephrine uptake-1 and norepinephrine uptake-2 inhibitor phenoxybenzamine (50 mg/kg intravenously; $n = 4$), the selective norepinephrine uptake-1 inhibitor desipramine (2 mg/kg intravenously; $n = 4$), or saline control (intravenously; $n = 4$). **Results:** ^{18}F -LMI1195 produced high and sustained heart uptake allowing clear delineation of the left ventricular wall over 60 min after tracer administration. Pretreatment with phenoxybenzamine markedly reduced the ^{18}F -LMI1195 cardiac uptake when compared with controls. In contrast, there was preserved ^{18}F -LMI1195 uptake after desipramine pretreatment. **Conclusion:** In rats, cardiac uptake of ^{18}F -LMI1195 was significantly inhibited by phenoxybenzamine but not desipramine, suggesting ^{18}F -LMI1195 is a substrate for the uptake-2 mechanism and is consistent with the rat heart having a dominant level of the mechanism.

Key Words: imaging; PET; sympathetic nerve; heart; norepinephrine; rat; NET

J Nucl Med 2013; 54:1142–1146

DOI: 10.2967/jnumed.112.104232

The sympathetic nervous system is an essential element for the regulation of cardiac function, adapting to the daily changing demands of physiologic conditions. It is well known that chronic hyperactivation of this system in patients with heart failure plays an important role in the vicious cycle of advanced disease pro-

gression by increasing myocardial energy requirements, afterload, and arrhythmias (1). Radionuclide imaging techniques provide noninvasive information about cardiac sympathetic innervation and nerve activity (2,3). These techniques uniquely facilitate understanding of the local cardiac sympathetic nervous system in physiologic and pathologic conditions, in contrast to blood tests, which only assess systemic sympathetic conditions.

Most commonly used for cardiac sympathetic nerve imaging are norepinephrine analog tracers, including ^{123}I -metaiodobenzylguanidine for SPECT and ^{11}C -hydroxyephedrine for PET (2–5). The PET assay is superior to SPECT in terms of quantification and temporal and spatial resolution. However, the clinical application of ^{11}C -hydroxyephedrine is limited because of the short radioactive half-life of ^{11}C (~20 min), which requires costly on-site cyclotron-dependent radionuclide production for the tracer synthesis and also has limitations for catecholamine turnover assessment by delayed scans. On the other hand, ^{18}F PET tracers, which have a longer radioactive half-life of approximately 110 min, have a significant potential to overcome the disadvantages of conventional ^{11}C -labeled sympathetic nerve PET imaging tracers by distribution of the tracer from a central cyclotron facility in a manner similar to ^{18}F -FDG (6). Additionally, this class of tracers may provide higher flexibility in the design of study protocols using delayed or prolonged imaging, possibly contributing to the broader application of this methodology in research and clinical applications (6–9). However, there are no clinically established ^{18}F -labeled sympathetic nerve PET tracers yet.

Recently, a novel ^{18}F -labeled PET tracer, LMI1195 (*N*-[3-bromo-4-(3- ^{18}F -fluoropropoxy)-benzyl]-guanidine), was introduced. This tracer, based on a benzylguanidine structure, shares similarities with the clinically established sympathetic nerve SPECT tracer ^{123}I -metaiodobenzylguanidine. Initial characterization of this new compound has been reported by Yu et al. (10). High human norepinephrine transporter binding affinity was proven by experiments using cell membranes overexpressing human norepinephrine transporter and human neuroblastoma cells (10). Furthermore, by performing *in vivo* norepinephrine neural uptake-1 blocking experiments with desipramine in New Zealand White rabbits and nonhuman primates, resulting in significant cardiac tracer uptake reduction, a high selectivity for norepinephrine transporters was proven.

Rat models have been the most widely and successfully used heart failure models in basic and translational research (11). However, it is known that there are significant species differences in the existence of norepinephrine uptake mechanisms in rat hearts, compared with primate hearts (12–15). Therefore, the aim of this study

Received Oct. 16, 2012; revision accepted Nov. 29, 2012.

For correspondence contact: Takahiro Higuchi, Comprehensive Heart Failure Center /Department of Nuclear Medicine, Würzburg University, Oberduerrbacher Strasse 6, D-97080 Würzburg, Germany.

E-mail: higuchi_t@klinik.uni-wuerzburg.de

Published online May 13, 2013.

COPYRIGHT © 2013 by the Society of Nuclear Medicine and Molecular Imaging, Inc.

was to investigate the mechanisms of the PET tracer ^{18}F -LMI1195 uptake in the rat hearts.

MATERIALS AND METHODS

Animals

In all of our experiments, healthy male Wistar rats weighting 250–300 g were used. Experimental protocols were approved by the regional governmental commission of animal protection (Regierung von Oberbayern, Germany) and conformed to the guidelines of the U.S. National Institutes of Health.

Tracer Production and Experimental Protocols

Synthesis and quality control of ^{18}F -LMI1195 were performed using a previously described procedure (10). ^{18}F -LMI1195, with a radiochemical purity of 98% or more and specific activity of 600 GBq/ μmol or more, was used in the biologic evaluation and small-animal PET studies.

Two series of experiments were performed (Fig. 1). The first protocol was designed to assess the systemic and myocardial tracer distribution of ^{18}F -LMI1195 over 60 min ($n = 4$). Shortly before an injection of 37 MBq of ^{18}F -LMI1195 via the tail vein, a dynamic PET scan for an interval of 60 min was initiated (Fig. 1). The second protocol was designed to evaluate the cardiac ^{18}F -LMI1195 uptake mechanism. Animals were pretreated with phenoxybenzamine (50 mg/kg intravenously; nonselective blockage of neural uptake-1 and nonneural uptake-2) (Sigma Aldrich Co.), desipramine (2 mg/kg intravenously; selective blockage of neural uptake-1) (Sigma Aldrich Co.), or 0.9% saline as a control group. Ten minutes after these respective pretreatments, 37 MBq of ^{18}F -LMI1195 were administered via the tail vein. A 10-min dynamic PET session was started shortly before the tracer injection. Animals were euthanized immediately after the imaging sessions; hearts and blood were obtained for ex vivo analysis with autoradiography (CR35 Bio; Raytest) and γ -counter (Wallac 1480-011 Automatic γ -Counter; PerkinElmer).

PET Acquisition and Reconstruction

All animals were maintained anesthetized during the whole experiment by 2% isoflurane. All scans were obtained using a dedicated small-animal PET/CT system (Inveon microPET/CT; Siemens Pre-clinical Solutions). The animals were placed prone on the PET/CT gantry, and CT images of the chest were acquired. CT data were acquired with the voltage set to 80 kV, a tube current of 500 μA , and a total rotation angle of 220° with 121 projections. CT data were

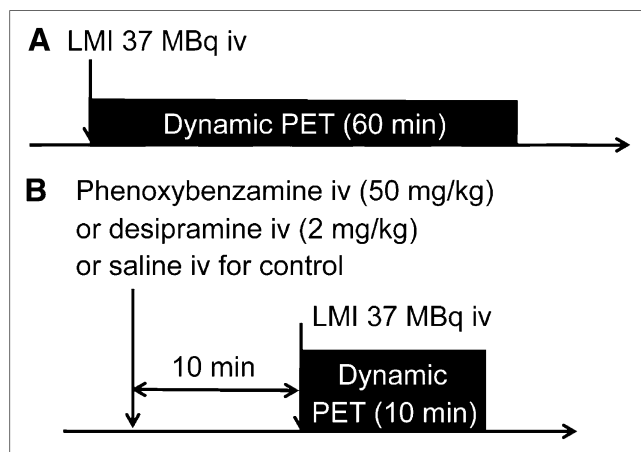


FIGURE 1. Schematic diagram illustrating protocols for PET imaging. iv = intravenous injection; LMI = ^{18}F -LMI1195.

reconstructed using filtered backprojection with the Shepp filter set to the Nyquist frequency, followed by PET image acquisition in list-mode format. The data were sorted into 3-dimensional sinograms, which were then rebinned with a Fourier algorithm to reconstruct dynamic images using a 2-dimensional ordered-subset expectation maximization algorithm. The reconstructed dynamic images consisted of the following frames: 12×15 s, 7×60 s, and 5×10 min adding up to 1 h and 12×15 and 7×60 s adding up to 10 min. All images were corrected for ^{18}F decay, randoms, and dead time; correction for attenuation was not performed.

PET Data Analysis

The obtained PET images were analyzed with the public domain tool AMIDE imaging software (version 1.01). Time-activity curves were generated using 3-dimensional regions of interest, which were manually placed in the myocardium, blood pool (left ventricle), lung, liver, kidney, adrenal glands, bone, and muscle. The mean radioactivity concentration within the region of interest was converted to Becquerels per centimeter cubed and expressed as percentage injected dose per centimeter cubed ($\%/\text{ID}/\text{cm}^3$).

Statistics

Data were presented as mean \pm SD. Comparison of continuous variables between multiple groups was performed by ANOVA using ranks (Kruskal–Wallis test), followed by the Dunn multiple-contrast hypothesis test to identify different pairs of groups. A value of P less than 0.05 was considered statistically significant. Statistical analysis was performed with StatMate III (ATMS Co., Ltd.).

RESULTS

^{18}F -LMI1195 Distribution

Figure 2 shows the time course of the systemic ^{18}F -LMI1195 distribution by in vivo PET analysis of healthy rats over 60 min after tracer injection.

Cardiac uptake including left ventricular blood-pool activity of ^{18}F -LMI1195 was discriminable in the first frame after tracer injection (0–3 min). On the second frame image (3–10 min), the left ventricular wall was clearly delineable from the blood pool because of the rapid clearance of blood tracer activity. The left ventricular wall remained clearly visible until the end of the last frame (50–60 min). The time-activity curve analysis of the absolute tracer concentration in the myocardium showed a high and stable tracer activity (~ 2 $\%/\text{ID}/\text{cm}^3$) throughout the scan time of 60 min, with minimal washout over time (0.4% per min).

Regional ^{18}F -LMI1195 distribution in the healthy myocardium by in vivo PET and ex vivo autoradiography is demonstrated in Figure 3. In vivo PET showed homogeneous tracer uptake throughout the left ventricular wall. Ex vivo autoradiography proved there was homogeneous tracer uptake into the myocardium, including the right ventricular wall. Lack of delineation of the right ventricular wall by in vivo PET might be due to the partial-volume artifact caused by the thinness of the right ventricular wall.

Notably, ^{18}F -LMI1195 liver uptake remained low, compared with the heart, facilitating the evaluation of inferior wall activity. Slightly increased bone activity in later frames was observed, suggesting the presence of some free ^{18}F -fluoride, a possible metabolite from ^{18}F -LMI1195. Renal excretion of ^{18}F -LMI1195 tracer activity is indicated by the transitional high renal tracer uptake.

Cardiac Uptake Blocking

Figure 4 shows the PET results of blockage of the nonselective neural uptake-1 and nonneural uptake-2 mechanism with

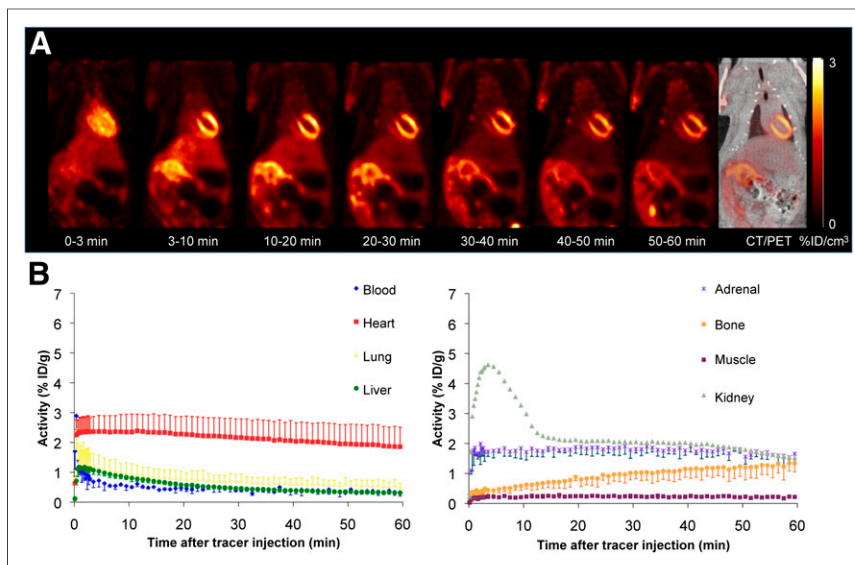


FIGURE 2. (A) Example of dynamic PET/CT image in coronal section of healthy rat using ^{18}F -LMI1195 at different time points after tracer injection. (B) Average time-activity curves of different organs assessed by PET imaging. Stable increase of cardiac ^{18}F -LMI1195 uptake throughout whole scan can be observed.

phenoxybenzamine and the selective blockage of the neural uptake-1 mechanism with desipramine on myocardial ^{18}F -LMI1195 uptake in healthy rat hearts. Treatment with phenoxybenzamine (50 mg/kg intravenously) decreased the myocardial ^{18}F -LMI1195 uptake, whereas treatment with desipramine (2 mg/kg intravenously) did not change myocardial ^{18}F -LMI1195 uptake, compared with the untreated control group. Myocardial tracer concentration 10 min after tracer injection was $2.35 \pm 0.59\% \text{ID}/\text{cm}^3$ in the control group, $1.20 \pm 0.04\% \text{ID}/\text{cm}^3$ (vs. control, $P < 0.001$) in the phenoxybenzamine group, and $2.59 \pm 0.37\% \text{ID}/\text{cm}^3$ in the desipramine group (vs. control, $P =$ not significant).

DISCUSSION

This study indicates a potential use for the novel ^{18}F -labeled tracer ^{18}F -LMI1195 in the imaging of norepinephrine uptake in rat hearts. There was a clear delineation of the left ventricular myocardium in healthy animals, with minimal tracer washout as shown by 1-h dynamic in vivo PET. Moreover, low tracer uptake in the liver is beneficial for evaluating the inferior wall tracer uptake without scatter artifact. ^{18}F -LMI1195 is also specific for cardiac norepinephrine uptake, as proven by blocking studies with phenoxybenzamine, a nonselective norepinephrine uptake-1 and -2 blocker (16,17). However, different from the previously reported studies with rabbit and nonhuman primate hearts (10), we found no reduction of cardiac ^{18}F -LMI1195 uptake by selective neural uptake-1 blocker (12) pretreatment with desipramine in rats, suggesting a significant contribution of the nonselective uptake-2 mechanism to cardiac ^{18}F -LMI1195 uptake in the rat heart. Although neural norepinephrine uptake-1 is the major mechanism of norepinephrine handling in nerve terminals reflecting sympathetic nerve activity, the nonneural uptake-2 mechanism also contributes to the removal of norepinephrine from the synaptic cleft and changes in pathologic conditions (12,16,18). Recently, it has been suggested that the nonneural uptake-2 mechanism is involved in provoking arrhythmias and in the progression of heart failure

(16,18–20). Therefore, these results imply that ^{18}F -LMI1195 has the potential to be a new class of assay to facilitate research into the understanding of cardiac norepinephrine uptake-2 mechanism in various heart diseases and might be used for monitoring the effects of medication on the norepinephrine uptake in rat models.

Several ^{18}F -labeled tracers for sympathetic nerve imaging, including ^{18}F -meta-raminol, ^{18}F -3,4-dihydroxyphenylalanine, and ^{18}F -labeled benzylguanidines, have been reported to offer the potential for imaging the sympathetic nervous system but have to be further established in terms of synthesis simplicity and tracer specificity before introduction into the broader clinical application (21–23). ^{18}F -LMI1195 is another recently introduced ^{18}F -labeled PET tracer for sympathetic nerve imaging based on a benzylguanidine structure that shares similarities with ^{123}I -metaiodobenzylguanidine. ^{18}F -LMI1195 can be synthesized by a single-step nucleophilic substitution reaction, followed by a high-

performance liquid chromatography purification with a high radiochemical yield. Yu et al. reported the initial evaluation of this novel tracer in cells and animal models (10). The affinity and uptake kinetics of ^{18}F -LMI1195 were similar to those of norepinephrine in vitro experiments using human norepinephrine transporter over-expressing cell membranes and human neuroblastoma cells. The specificity of the cardiac ^{18}F -LMI1195 uptake for neural uptake-1 mechanism was studied in rabbits and nonhuman primates using the selective neural uptake-1 blocker desipramine. Pretreatment with a maximum of 1 mg/kg reduced the cardiac

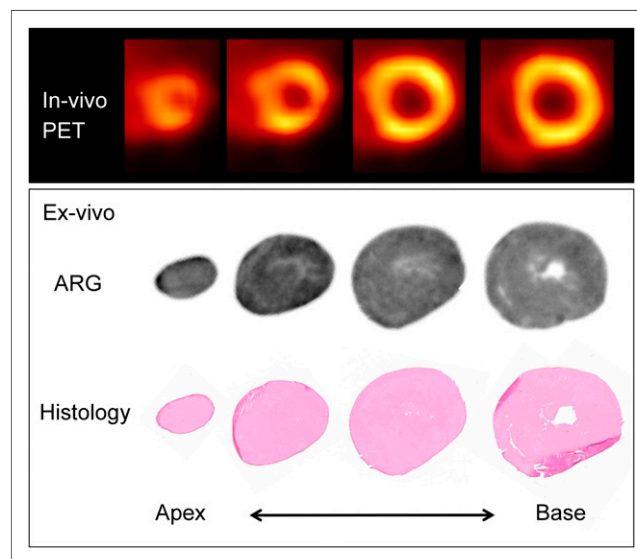


FIGURE 3. Short-axis heart images from healthy rat by in vivo ^{18}F -LMI1195 PET (top), ex vivo ^{18}F -LMI1195 autoradiography (middle), and hematoxylin and eosin staining (bottom). Homogeneous ^{18}F -LMI1195 distribution throughout left ventricular wall can be seen. ARG = autoradiography.

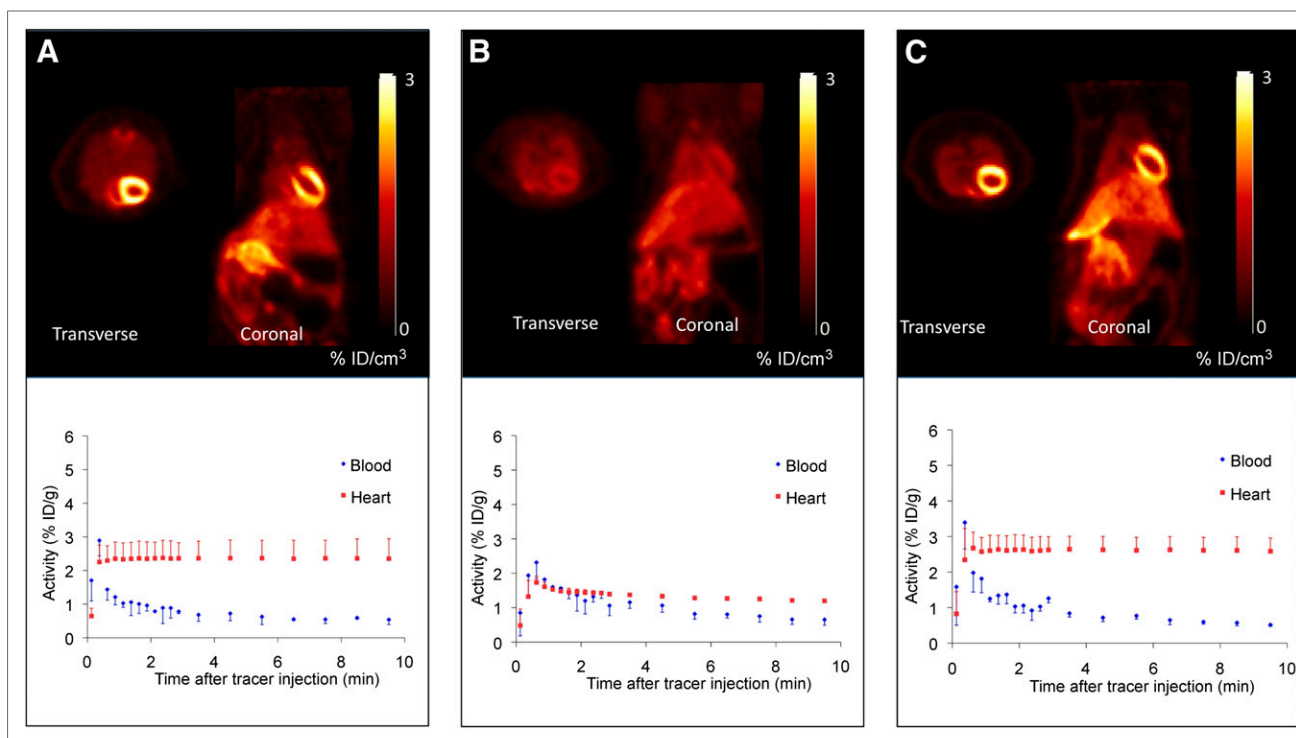


FIGURE 4. Example coronal and transverse in vivo ^{18}F -LMI1195 PET images (upper) and averaged time–activity curves of 10-min dynamic PET acquisition (lower) after different pretreatments: control saline (A), 50 mg/kg dose of phenoxybenzamine (B), and 2 mg/kg dose of desipramine (C). Significant reduction of cardiac ^{18}F -LMI1195 uptake is seen after phenoxybenzamine treatment.

^{18}F -LMI1195 uptake in rabbits by approximately 82%, whereas ^{123}I -metaiodobenzylguanidine heart uptake was reduced by approximately 53% using the same protocol; the results in non-human primates showed a similar pattern. These experimental results indicate that ^{18}F -LMI1195 might allow for highly specific cardiac neural imaging in human hearts using PET. Furthermore, in a clinical phase 1 study, increased myocardial uptake and tolerability with radiation dose comparable to that of other commonly used PET tracers in humans were suggested, warranting further clinical phase 2 studies to elucidate its potential applications in patients with heart diseases (24,25).

The focus of the present study was to investigate the cardiac ^{18}F -LMI1195 uptake mechanism in rat hearts. Although the rat is one of the most commonly used animals for heart failure models (11), it has been reported to have significant variations in myocardial norepinephrine handling, compared with human and other species, including the high existence of nonneural uptake-2 mechanism (12–15). After the release of norepinephrine from the synapse, removal of norepinephrine from the cleft, an important process for terminating the norepinephrine-mediated sympathetic nerve stimulation, is mainly attributed to 2 different mechanisms. One is the reuptake of norepinephrine by the neural uptake-1 transporter back into the synapse for subsequent reuse. The second mechanism is the nonneural uptake-2 into the myocytes, followed by degradation by catechol-*O*-methyltransferase and monoamine oxidase, which has lower affinity to norepinephrine than to the uptake-1 mechanism. In rat hearts, Fiebig et al. demonstrated a significantly high contribution to the norepinephrine removal from the nerve terminal via the uptake-2 mechanism equal to that of the uptake-1 mechanism, especially in the presence of relatively low concentrations of norepinephrine (13,26).

Desipramine is one of the most commonly used selective uptake-1 blocking agents. The precise complex structure and molecular mechanism of inhibition of the norepinephrine transporter, the molecule responsible for neural uptake-1, by desipramine has been identified recently (27). The successful reduction in uptake of the cardiac ^{11}C -labeled PET tracer ^{11}C -hydroxyephedrine in rat hearts using the same blockage protocol (a 2 mg/kg dose of desipramine 10 min before tracer administration) has been reported (28). On the other hand, cardiac uptake of the SPECT tracer ^{123}I -metaiodobenzylguanidine was preserved in the same way as ^{18}F -LMI1195 in the present data (28). ^{18}F -LMI1195 and ^{123}I -metaiodobenzylguanidine share a benzylguanidine-analog structure, possibly explaining the similarity of response to the blocker. It stands to reason that in addition to the species variations for the norepinephrine uptake mechanisms, affinity differences relating to structure may exist between the neural uptake-1 and nonneural uptake-2 mechanisms.

Iversen et al. were the first to describe the second norepinephrine uptake pathway, the nonneural uptake-2 mechanism, in isolated rat heart experiments, in 1965 (12). Recently, the transporter OCT3 has been identified to be the mediator of the nonneural uptake-2 mechanism (29,30). Potent inhibitors for this mechanism include metanephrine (31,32), steroids (33), and phenoxybenzamine (17,34). The substance we used in our experiments, phenoxybenzamine, is based on a haloalkylamide structure and is reported to be a highly potent and irreversible inhibitor of the uptake-2 mechanism; however, phenoxybenzamine also blocks the neural uptake-1 mechanism simultaneously (17). Therefore, to characterize the ^{18}F -LMI1195 uptake mechanism, we combined the nonselective phenoxybenzamine blocking experiments with selective neural uptake-1 blocking with desipramine to further elucidate the contribution of the uptake-2 mechanism.

CONCLUSION

There is a clear and stable delineation of the left ventricular wall using the novel ^{18}F -labeled benzylguanidine analog ^{18}F -LMI1195, indicating a feasibility to perform in vivo cardiac imaging in rat hearts. In contrast to the previous results of high ^{18}F -LMI1195 affinity to the neural uptake-1 mechanism by in vitro human norepinephrine transporter experiments and in vivo rabbit and non-human primate experiments, a high contribution of ^{18}F -LMI1195 uptake via the nonneural uptake-2 mechanism was found in rat hearts.

DISCLOSURE

The costs of publication of this article were defrayed in part by the payment of page charges. Therefore, and solely to indicate this fact, this article is hereby marked "advertisement" in accordance with 18 USC section 1734. No potential conflict of interest relevant to this article was reported.

REFERENCES

1. Parati G, Esler M. The human sympathetic nervous system: its relevance in hypertension and heart failure. *Eur Heart J*. 2012;33:1058–1066.
2. Higuchi T, Schwaiger M. Noninvasive imaging of heart failure: neuronal dysfunction and risk stratification. *Heart Fail Clin*. 2006;2:193–204.
3. Higuchi T, Schwaiger M. Imaging cardiac neuronal function and dysfunction. *Curr Cardiol Rep*. 2006;8:131–138.
4. Nguyen NT, DeGrado TR, Chakraborty P, Wieland DM, Schwaiger M. Myocardial kinetics of carbon-11-epinephrine in the isolated working rat heart. *J Nucl Med*. 1997;38:780–785.
5. DeGrado TR, Hutchins GD, Toorongian SA, Wieland DM, Schwaiger M. Myocardial kinetics of carbon-11-meta-hydroxyephedrine: retention mechanisms and effects of norepinephrine. *J Nucl Med*. 1993;34:1287–1293.
6. Rischpler C, Park MJ, Fung GS, Javadi M, Tsui BM, Higuchi T. Advances in PET myocardial perfusion imaging: F-18 labeled tracers. *Ann Nucl Med*. 2012;26:1–6.
7. Higuchi T, Nekolla SG, Huisman MM, et al. A new ^{18}F -labeled myocardial PET tracer: myocardial uptake after permanent and transient coronary occlusion in rats. *J Nucl Med*. 2008;49:1715–1722.
8. Huisman MC, Higuchi T, Reder S, et al. Initial characterization of an ^{18}F -labeled myocardial perfusion tracer. *J Nucl Med*. 2008;49:630–636.
9. Nekolla SG, Reder S, Saraste A, et al. Evaluation of the novel myocardial perfusion positron-emission tomography tracer ^{18}F -BMS-747158-02: comparison to ^{13}N -ammonia and validation with microspheres in a pig model. *Circulation*. 2009;119:2333–2342.
10. Yu M, Bozek J, Lamoy M, et al. Evaluation of LMI1195, a novel ^{18}F -labeled cardiac neuronal PET imaging agent, in cells and animal models. *Circ Cardiovasc Imaging*. 2011;4:435–443.
11. Patten RD, Hall-Porter MR. Small animal models of heart failure: development of novel therapies, past and present. *Circ Heart Fail*. 2009;2:138–144.
12. Iversen LL. The uptake of catechol amines at high perfusion concentrations in the rat isolated heart: a novel catechol amine uptake process. *Br J Pharmacol Chemother*. 1965;25:18–33.
13. Carr EA Jr., Carroll M, Counsell RE, Tyson JW. Studies of uptake of the bretylium analogue, iodobenzyltrimethylammonium iodide, by non-primate, monkey and human hearts. *Br J Clin Pharmacol*. 1979;8:425–432.
14. Paczkowski FA, Bryan-Lluka LJ, Porzgen P, Bruss M, Bonisch H. Comparison of the pharmacological properties of cloned rat, human, and bovine norepinephrine transporters. *J Pharmacol Exp Ther*. 1999;290:761–767.
15. Jarrott B. Uptake and metabolism of catecholamines in the perfused hearts of different species. *Br J Pharmacol*. 1970;38:810–821.
16. Solbach TF, Grube M, Fromm MF, Zolk O. Organic cation transporter 3: expression in failing and nonfailing human heart and functional characterization. *J Cardiovasc Pharmacol*. 2011;58:409–417.
17. Iversen LL, Salt PJ, Wilson HA. Inhibition of catecholamine uptake in the isolated rat heart by haloalkylamines related to phenoxybenzamine. *Br J Pharmacol*. 1972;46:647–657.
18. Babin-Ebell J, Gliese M. Extraneuronal uptake of noradrenaline in human tissue (uptake2). *Heart Vessels*. 1995;10:151–153.
19. Grube M, Ameling S, Noutsias M, et al. Selective regulation of cardiac organic cation transporter novel type 2 (OCTN2) in dilated cardiomyopathy. *Am J Pathol*. 2011;178:2547–2559.
20. Schroeder C, Jordan J. Norepinephrine uptake mechanisms in cardiovascular disease deserve our attention. *J Cardiovasc Pharmacol*. 2011;58:406–408.
21. Kopka K, Schober O, Wagner S. ^{18}F -labelled cardiac PET tracers: selected probes for the molecular imaging of transporters, receptors and proteases. *Basic Res Cardiol*. 2008;103:131–143.
22. Mislankar SG, Gildersleeve DL, Wieland DM, Massin CC, Mulholland GK, Toorongian SA. 6- ^{18}F fluorometaraminol: a radiotracer for in vivo mapping of adrenergic nerves of the heart. *J Med Chem*. 1988;31:362–366.
23. Raffel DM, Jung YW, Gildersleeve DL, et al. Radiolabeled phenethylguanidines: novel imaging agents for cardiac sympathetic neurons and adrenergic tumors. *J Med Chem*. 2007;50:2078–2088.
24. Lazewatsky J, Sinusas A, Brunetti J, et al. Radiation dosimetry of LMI1195, first-in-human study of a novel F-18 labeled tracer for imaging myocardial innervation [abstract]. *J Nucl Med*. 2010;51(suppl 2):1432.
25. Liu Y-H, Srivastava A, Mulnix T, et al. Quantification of normal pattern of regional myocardial uptake of ^{18}F LMI1195, a novel tracer for imaging myocardial sympathetic function: first-in-human study [abstract]. *J Nucl Med*. 2010;51(suppl 2):1317.
26. Fiebig ER, Trendelenburg U. The neuronal and extraneuronal uptake and metabolism of ^3H -(-)-noradrenaline in the perfused rat heart. *Naunyn Schmiedeberg Arch Pharmacol*. 1978;303:21–35.
27. Zhou Z, Zhen J, Karpowich NK, et al. LeuT-desipramine structure reveals how antidepressants block neurotransmitter reuptake. *Science*. 2007;317:1390–1393.
28. Rischpler C, Fukushima K, Isoda T, et al. Discrepant uptake of the sympathetic nerve imaging tracers hydroxyephedrine (HED) and metaiodobenzylguanidine (MIBG) in rat hearts. *Circulation*. March 29, 2013 [Epub ahead of print].
29. Wu X, Kekuda R, Huang W, et al. Identity of the organic cation transporter OCT3 as the extraneuronal monoamine transporter (uptake2) and evidence for the expression of the transporter in the brain. *J Biol Chem*. 1998;273:32776–32786.
30. Gründemann D, Schechinger B, Rappold GA, Schomig E. Molecular identification of the corticosterone-sensitive extraneuronal catecholamine transporter. *Nat Neurosci*. 1998;1:349–351.
31. Picken GM, Jarrott B. Effects of blockade of extraneuronal uptake on responses to isoprenaline in perfused rat heart. *Clin Exp Pharmacol Physiol*. 1975;2:249–259.
32. Tumer N, Mortimer ML, Roberts J. Gender differences in the effect of age on adrenergic neurotransmission in the heart. *Exp Gerontol*. 1992;27:301–307.
33. Iversen LL, Salt PJ. Inhibition of catecholamine uptake-2 by steroids in the isolated rat heart. *Br J Pharmacol*. 1970;40:528–530.
34. Hayer-Zillgen M, Bruss M, Bonisch H. Expression and pharmacological profile of the human organic cation transporters hOCT1, hOCT2 and hOCT3. *Br J Pharmacol*. 2002;136:829–836.